Since January 2020 Elsevier has created a COVID-19 resource centre with free information in English and Mandarin on the novel coronavirus COVID-19. The COVID-19 resource centre is hosted on Elsevier Connect, the company's public news and information website.

Mathematical Biosciences 358 (2023) 108970

Contents lists available at ScienceDirect

Mathematical Biosciences

journal homepage: www.elsevier.com/locate/mbs

Original Research Article

A mathematical model of protein subunits COVID-19 vaccines

Samaneh Gholami [a,*], Chapin S. Korosec [a], Suzan Farhang-Sardroodi [b,a], David W. Dick [a], Morgan Craig [c], Mohammad Sajjad Ghaemi [d], Hsu Kiang Ooi [d], Jane M. Heffernan [a]

[a] Modelling Infection & Immunity Lab, Centre for Disease Modelling, Mathematics & Statistics, York University, Toronto, Ontario, Canada
[b] Department of Mathematics, University of Manitoba, Winnipeg, Manitoba, Canada
[c] Sainte-Justine University Hospital Research Centre and Department of Mathematics and Statistics, Université de Montréal, Montreal, Quebec, Canada
[d] Digital Technologies Research Centre, National Research Council Canada, Toronto, ON, Canada

ARTICLE INFO

Keywords:
Protein subunit-based vaccine
SARS-CoV-2
COVID-19
Adaptive immune response
Neutralizing Antibody (NAb)
IgG antibody
Mathematical modeling

ABSTRACT

We consider a general mathematical model for protein subunit vaccine with a focus on the MF59-adjuvanted spike glycoprotein-clamp vaccine for SARS-CoV-2, and use the model to study immunological outcomes in the humoral and cell-mediated arms of the immune response from vaccination. The mathematical model is fit to vaccine clinical trial data. We elucidate the role of Interferon-γ and Interleukin-4 in stimulating the immune response of the host. Model results, and results from a sensitivity analysis, show that a balance between the T_H1 and T_H2 arms of the immune response is struck, with the T_H1 response being dominant. The model predicts that two-doses of the vaccine at 28 days apart will result in approximately 85% humoral immunity loss relative to peak immunity approximately 6 months post dose 1.

1. Introduction

Several COVID-19 vaccines have been approved for use in the global population, to mitigate the effect of the pandemic. The robustness of current vaccines with respect to the generation of long term immunity remains to be elucidated. In the current study, we continue previous work on SARS-Cov-2 mRNA based [1,2] and Adenovirus [3] vaccines to quantify the effects of a protein-based subunit vaccine in immunity generation and longevity.

Our study is based upon data from the MF59-adjuvanted spike glycoprotein-clamp vaccine [4]. In general, protein based subunit vaccines present an antigen to the immune system using a specific, isolated protein of the pathogen. As the protein subunit vaccine does not replicate in the host, there is no risk of pathogenicity (ability of an organism to cause disease) [5]. Early studies of protein subunit vaccines demonstrated low immunogenicity (inability to activate T helper (T_H) cells) [6]. Adjuvants are thus added to protein subunit vaccine formulations to enhance the magnitude and durability of the immune response [7–9]. Protein subunit vaccines generally include a coupling of an antigen to a protein that transforms the antigen into a thymus dependent antigen capable of eliciting immunoglobulin G (IgG) and memory responses. Adjuvanted subunit vaccines have been licensed for as a prophylactic measure against disease such as Pneumococcus, Neisseria meningitidis and Haemophilus influenza type b (Hib) [10,11].

The MF59-adjuvanted spike glycoprotein-clamp vaccine [4] consists of a recombinant SARS-CoV-2 spike glycoprotein and the adjuvant MF59. The MF59 is a squalene oil-in-water emulsion that it is an FDA-approved adjuvant with a long track record of safety across all age cohort [4]. A molecular sclamp is used to stabilize the spike glycoprotein to allow for maximal immune system activation. Phase 1 clinical trials of this vaccine included different dose levels, at 5, 15, and 45 μg, in a two-dose regimen, and a single dose of vaccine at 45 μg followed by placebo. The vaccine was administered intramuscularly 28 days apart. Clinical trial subjects had blood samples collected on day 15, 43, and 57. Details of the clinical trial are provided in [4].

To study the activation and durability of immunity after administration of MF59-adjuvanted spike glycoprotein-clamp vaccine, we develop a system of ordinary differential equations (ODE) that describes the humoral and cell-mediated immune response to protein subunit vaccines and adjuvants. We fit our model to cytokines and immune cell data from the vaccine clinical trial using two doses of 45 μg MF59-adjuvanted spike glycoprotein- clamp vaccine in humans [4]. The model is used to project humoral immunity loss over three months from dose one of the vaccine and consider a Th1:Th2 balance of the immune response. Following the main analysis, we consider five plausible immune adjuvant stimulation scenarios of the humoral immune response that can inform future development of adjuvants. A sensitivity analysis is performed to identify model parameters that have maximum effect on the peak magnitude of the immune response and immunity loss. Results point to increased sensitivity to parameters in the T_H1 component of the immune response.

* Corresponding author.
E-mail address: sama20@yorku.ca (S. Gholami).

https://doi.org/10.1016/j.mbs.2023.108970
Received 2 February 2022; Received in revised form 21 January 2023; Accepted 22 January 2023
Available online 10 February 2023

2. Method

2.1. Clinical data acquisition

An MF59-adjuvanted subunit vaccine for COVID-19 based on recombinant SARS-CoV-2 spike glycoprotein was studied in [4]. The spike glycoprotein was stabilized in a prefusion conformation by a novel molecular clamp (Sclamp) [4]. The vaccine contained recombinant SARS-CoV-2 glycoprotein and squalene oil-in-water adjuvant (MF59). The clinical trial was conducted in Australia. 120 healthy adults (18–55 years) received two doses of placebo, 5-μg, 15-μg, or 45-μg SARS-CoV-2 Sclamp, or one 45-μg dose of SARS-CoV-2 Sclamp followed by placebo (24 per group). The clinical trial doses were administered intramuscularly 28 days apart. Clinical trial subjects had blood samples collected on day 15, 43, and 57. Measurements of neutralizing antibodies (nAB), the Ig-multiplex (a detailed description in the supplemental text.), T_H1 cytokines (IFN_γ, TNF_β and IL-2) T_H2 cytokines (IL-4 and IL-13), cytotoxic T-lymphocytes CTL, Interferon-γ (IFN_γ), and Interleukin-4 (IL4) were determined at each time point [4].

Pooled data of the 15-μg and 45-μg two-dose trial population were obtained from publicly accessible sources [4]. The pooled 45-μg clinical trial data is shown in Fig. 2 (red dots). This data is also shown along side pooled 15-μg two-dose clinical trial data and in the Supplementary Material.

2.2. Model

A mathematical model consisting of a system of ordinary differential equations (ODEs) is developed to describe the activation of the immune system by the protein subunit vaccine. The model is fit to the pooled data from multiple patients for the MF59-adjuvanted vaccine based on the recombinant spike protein [4]. Various effects of stimulating the immune system with vaccine adjuvant are analyzed in this work.

We developed a general adjuvanted protein subunit vaccine induced immune response model. The mathematical model describes the dynamics of the vaccine and the immune response. The model considers vaccine particles [V], and different components of the innate, humoral and cell-mediated arms of the immune system, including T_H1 Cytokines [Th1], T_H2 Cytokines [Th2], Interferon-γ [F], Interleukin-4 [I4], Cytotoxic T cells [CTL], Neutralizing Antibody [A] and an Ig-antibody multiplex [B] which denotes the combination of Early (IgM) + Late Antibodies (IgG). A flow diagram of the model is shown in Fig. 1. Table 1 lists the model parameters and definitions. The system of ordinary differential equations is as follows:

$$\frac{d[V]}{dt} = -(1+\psi)\eta_v[V][A] - \gamma_v[V] \tag{1a}$$

$$\frac{d[Th1]}{dt} = (1+\psi)\eta_{th1}[V] + \eta_{th1_f}[F] - \beta_{th1_{i4}}[Th1]\frac{[I4]}{k_{th1}+[I4]} - \gamma_{th1}[Th1] \tag{1b}$$

$$\frac{d[Th2]}{dt} = (1+\psi)\eta_{th2}[V] + \eta_{th2_f}[F] - \beta_{th2_f}[Th2][F] - \gamma_{th2}[Th2] \tag{1c}$$

$$\frac{d[F]}{dt} = \eta_f[Th1] - \gamma_f[F] \tag{1d}$$

$$\frac{d[I4]}{dt} = \eta_{i4}[Th2] - \gamma_{i4}[I4] \tag{1e}$$

$$\frac{d[CTL]}{dt} = (1+\psi)\eta_{ctl}[V] + \eta_{ctl_f}[CTL]\frac{[F]}{k_{ctl}+[F]} - \gamma_{ctl}[CTL] \tag{1f}$$

$$\frac{d[A]}{dt} = \eta_a[B] - \gamma_a[A] \tag{1g}$$

$$\frac{d[B]}{dt} = \eta_{b_{th1}}[Th1] + \eta_{b_{th2}}[Th2] - \gamma_b[B] \tag{1h}$$

Briefly, the spike proteins on the vaccine [V] are recognized by the innate immune response and are presented to the adaptive immune response using antigen presenting cells (APCs). It is assumed that the APCs are proportional to the vaccine virus [V]. APCs stimulate CD4+, T helper cells and cytotoxic T-lymphocytes (CTL). We consider type 1 [Th1] and type 2 [Th2] T-helper cells cytokines which are responsible for activating the humoral (T_H2) and cell-mediated (T_H2 and CTL) arms of the immune response [13,14]. The T_H1, T_H2 and CTL activation rates are given by η_{th1}, η_{th2}, and η_{ctl}, respectively. The T_H1 and T_H2 immune responses are distinguished by different panels of cytokines. Here, we give particular focus to IFN_γ [F], a pro-inflammatory T_H1 cytokine, and IL-4 [I4], a T_H2 cytokine that evokes a strong antibody response, as both [F] and [I4] measured in the clinical trial. It is assumed that [F] and [I4] production are linearly related to [Th1] and [Th2] with rates η_f and η_{i4}, respectively. IFN_γ plays an activation role of T_H1, T_H2 and CTL [15–17]. This is represented in $\eta_{th1_f}[F]$, $\eta_{th2_f}[F]$, and $\eta_{ctl_f}[F]$ terms in Eq.'s (1b), (1c) and (1f). As T_H1 and T_H2 cytokines also have inhibition roles on the other arm of the immune response, we assume that IFN_γ and IL-4 inhibit T_H2-cell and T_H1-cell differentiation, respectively [15,18–20]. The inhibition terms are denoted by $\beta_{th1_{i4}}[Th1]\frac{[I4]}{k_{th1}+[I4]}$ and $\beta_{th2_f}[Th2][F]$ in Eq.'s (1b) and (1c), where k_{th1} is a threshold constant.

The form of the saturating term [I4] /kth1+[I4] was chosen based on receptor/ligand binding kinetics of Th1 cells and IL-4, namely that IL-4 attaches to its receptors on the surface of CD4+ T cells to induce its effect. This is based on the usual Hill function dynamics, with a Hill coefficient set to 1 (also known as Michaelis–Menten kinetics) [21]. The mass-action term, $\beta_{th2_f}[Th2][F]$, in Eq. (1c) reflects simple homogeneous mixing of the subpopulations. We found that mass action describes the primary inhibition well and can capture the vaccine dynamics. [Th1], [Th2], [F], [I4] and [CTL] have natural degradation rates γ_{th1}, γ_{th2}, γ_f, γ_{i4} and γ_{ctl} respectively.

In our model we focus on two subclasses of antibodies, an Ig-multiplex [B] (the combination of IgG and IgM antibodies), and neutralizing antibodies [A]. IgM is the main antibody present during a

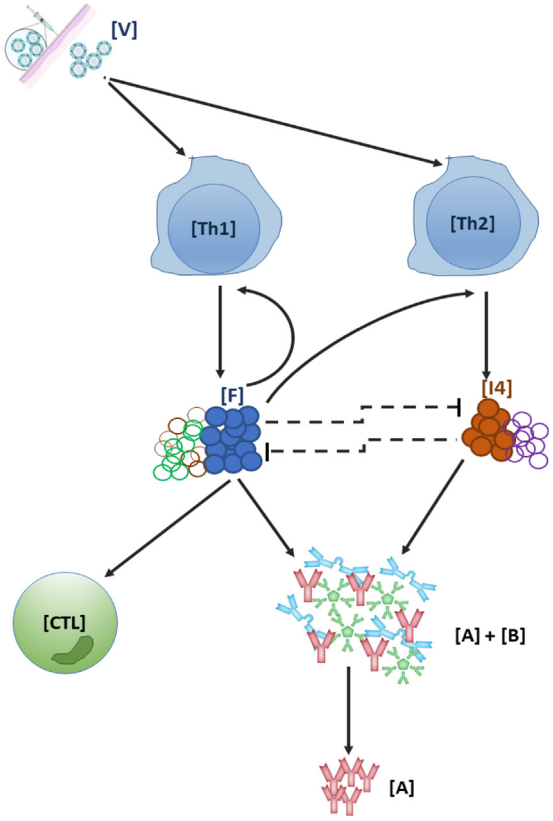

Fig. 1. Schematic model of intercellular interactions of adaptive immune system cells. V: Spike proteins on the vaccine, Th1: T_H1 cytokines, Th2: T_H2 cytokines, F: Interferon-γ, I4: Interleukin-4, CTL: Cytotoxic T-cell, A: Neutralizing antibodies, B: Ig-multiplex, The arrows denote cells, cytokines or antibodies production; bar-headed dash lines indicate suppressive intercellular interactions.

Table 1
Population fitted values of the model parameters for the two-dose MF59-adjuvanted spike glycoprotein-clamp vaccine. The parameters have units $(day)^{-1}$ except ψ, k_{th1}, k_{ctl} which are dimensionless.

Parameter	Definition	Value $(day)^{-1}$	Confidence interval	Comment
ψ	Adjuvant	0.0948	[0 , 0.388]	Fitted
η_v	Vaccine and antibody binding rate	1e−6	NA	[12]
γ_v	Vaccine clearance rate	0.75	[0.603 , 1.463]	Fitted
η_{th1}	T_H1 cytokines activation rate by vaccine	0.00678	[0.001 , 0.013]	Fitted
η_{th1_f}	T_H1 cytokines activation rate by interferon-γ	0.044	[0.039, 0.066]	Fitted
$\beta_{th1_{i4}}$	T_H1 cytokines inhibition rate by interleukin-4	0.85	[0.739 , 0.869]	Fitted
k_{th1}	T_H1 duplication threshold due to Interleukin-4	0.426	NA	Chosen
γ_{th1}	T_H1 cytokines clearance rate	0.000956	[0, 0.001]	Fitted
η_{th2}	T_H2 cytokines activation rate by vaccine	2.78e−5	[2.1e−05, 4.2e−05]	Fitted
η_{th2_f}	T_H2 cytokines activation rate by interferon-γ	0.017	[0.013 , 0.017]	Fitted
β_{th2_f}	T_H2 cytokines inhibition rate by interferon-γ	0.059	[0.002, 0.071]	Fitted
γ_{th2}	T_H2 cytokines clearance rate	0.07	[0, 0.152]	Fitted
η_f	Interferon-γ activation rate by T_H1	0.0181	[0.016 , 0.022]	Fitted
γ_f	Interferon-γ clearance rate	0.0796	[0.066 , 0.083]	Fitted
η_{i4}	Interleukin-4 activation rate by T_H2	0.138	[0.122 , 0.16]	Fitted
γ_{i4}	Interleukin-4 clearance rate	0.0913	[0.076 , 0.878]	Fitted
η_{ctl}	Cytotoxic T-cell activation rate by vaccine	800	[263.891 , 1503.92]	Fitted
η_{ctl_f}	Cytotoxic T-cell stimulation rate by Interferon-γ	110	[21.105 , 464.489]	Fitted
k_{ctl}	Cytotoxic T-cell duplication threshold rate due to interferon-γ	600	NA	[3]
γ_{ctl}	Cytotoxic T-cell clearance rate	0.026	[0.011 , 0.027]	Fitted
η_a	neutralizing antibody activation rate by Ig-multiplex	2.5	[1.049 , 2.985]	Fitted
γ_a	Neutralizing antibody clearance rate	0.90	[0.90 , 0.932]	Fitted
$\eta_{b_{th1}}$	Ig-multiplex activation rate by T_H1 cytokines	18	[16.118 , 21.935]	Fitted
$\eta_{b_{th2}}$	Ig-multiplex activation rate by T_H2 cytokines	6	[4.553 , 6.908]	Fitted
γ_b	Ig-multiplex clearance rate	0.05	[0.013 , 0.06]	Fitted

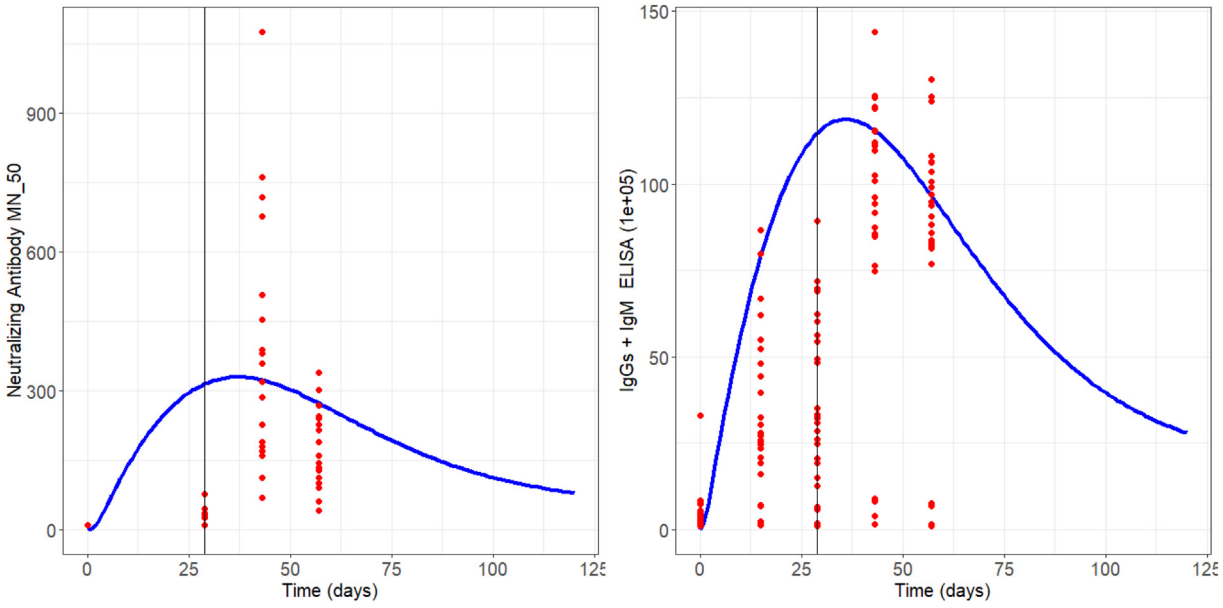

Fig. 2. Population fits (blue lines) to the neutralizing antibody and Ig-multiplex of the MF59-adjuvanted vaccine data (red dots) [4].

primary immune response, and IgG dominates during secondary immune responses and is the most common circulating antibody in the immune system [22,23]. Both IgG and IgM are elicited by T_H1 and T_H2 responses [24]. This is represented by $\eta_{b_{th1}}[Th1]$ and $\eta_{b_{th2}}[Th2]$ in Eq. (1h). It has been shown that SARS-CoV-2 IgG titres correlate with viral neutralization in humans [25]. We therefore model the increase in neutralization titres to be proportional to [B]. That is, we assume that neutralizing antibodies [A] are linearly proportional to the Ig-multiplex [B]. [A] and [B] have natural degradation rates γ_a and γ_b, respectively.

Adjuvants have been widely used in combination with many existing vaccines [26]. Model (1) was developed considering the documented effects of the M59-adjuvant on the T_H1 and T_H2 arms of the immune response [4]. Three different enhancement mechanisms are represented, namely, increases in the activation of the T_H1 (see Eq. (1b)) and T_H2 (see Eq. (1c)) immune responses related to cytokine activity, and increases in CTL activation (see Eq. (1f)). We also assume an increase the antibody binding rate, which can increase vaccine clearance in the system (see Eq. (1a)). We note that, for simplicity, we have included the adjuvant effect using the same parameter ψ in Eq.'s (1a)–(1c) and (1f). While the effect of the adjuvant can vary between the modeled mechanisms, this cannot be determined using the current data set. A more fine-grained study of the adjuvant is planned for future work.

2.3. Considering extensions of the adjuvant effect to [A] and [B] production

There are uncertainties around the effect of the adjuvant on antibody production. This has not been rigorously analyzed in Model (1). Models (2)–(6) (presented below) can replace Eq. (1g) and (1h) in Model (1) to allow for the consideration of adjuvant effects on [A]

and [B] production. Model (2) assumes that the adjuvant only affects production of [A]. Models (3) and (4) consider increased production of [B] by T_H1 and T_H2 activities, respectively. In Model (5), we consider increases in [B] production by both T_H1 and T_H2. Finally, Model (6) considers adjuvant augmentation in all [A] and [B] production terms. The inclusion of Models (2)–(6) allows for the study of T_H1 and T_H2 activity needed to enhance antibody production related to the adjuvant. Again, we note that, for simplicity we have included the adjuvant effect using the same parameter ψ in Eq.'s (1a)–(1c) and (1), and Models (2)–(6). While the effect of the adjuvant can vary between the models, the variability of the adjuvant mechanism for each model cannot be determined using the current data set. A more fine-grained study of the adjuvant is planned for future work.

Model 2:

$$\frac{d[A]}{dt} = (1+\psi)\eta_a[B] - \gamma_a[A] \tag{2a}$$

$$\frac{d[B]}{dt} = \eta_{bth1}[Th1] + \eta_{bth2}[Th2] - \gamma_b[B] \tag{2b}$$

Model 3:

$$\frac{d[A]}{dt} = \eta_a[B] - \gamma_a[A] \tag{3a}$$

$$\frac{d[B]}{dt} = (1+\psi)\eta_{bth1}[Th1] + \eta_{bth2}[Th2] - \gamma_b[B] \tag{3b}$$

Model 4:

$$\frac{d[A]}{dt} = \eta_a[B] - \gamma_a[A] \tag{4a}$$

$$\frac{d[B]}{dt} = \eta_{bth1}[Th1] + (1+\psi)\eta_{bth2}[Th2] - \gamma_b[B] \tag{4b}$$

Model 5:

$$\frac{d[A]}{dt} = \eta_a[B] - \gamma_a[A] \tag{5a}$$

$$\frac{d[B]}{dt} = (1+\psi)\eta_{bth1}[Th1] + (1+\psi)\eta_{bth2}[Th2] - \gamma_b[B] \tag{5b}$$

Model 6:

$$\frac{d[A]}{dt} = (1+\psi)\eta_a[B] - \gamma_a[A] \tag{6a}$$

$$\frac{d[B]}{dt} = (1+\psi)\eta_{bth1}[Th1] + (1+\psi)\eta_{bth2}[Th2] - \gamma_b[B] \tag{6b}$$

2.4. Parameter values

We parameterize the model by setting some parameter values and determining others through fitting of Model (1) to the vaccine clinical trial data of two 45 μg-adjuvanted vaccine doses [4], including data collected at three time points (day 15, 43 and 57) with > 22 samples at each time-point. Model fitting to the clinical trial data of two 15 μ_g-adjuvanted vaccine doses is also conducted, and is presented in the Supplementary Material.

To ensure parameter identifiability, we fixed a number of parameters whose values are informed by the literature. These informed values are listed in Table 1, including related references to the literature.

Parameter k_{th1}, representing the saturation of Interleukin-4 is chosen based on the half-max of the data set [27–29]. Fitted parameter values are determined through model fitting to clinical trial measurements of neutralizing antibodies, the Ig-multiplex, T_H1 cytokines, T_H2 cytokines, cytotoxic T-lymphocytes CTL, Interferon-γ (IFN_γ), and Interleukin-4 (IL4) [4]. The clinical trial data is shown in Fig. 2 (red dots) and in the Supplementary Material. Fitted parameters are estimated by computing the maximum likelihood estimator using the stochastic approximation expectation–maximization (SAEM) algorithm implemented in Monolix Software. This method has been proven to efficiently converge to the maximum likelihood estimator for nonlinear mixed effects models [30]. We assume that parameters follow a log-normal distribution.

Fitting assessment

Data fitting was performed using Monolix, developed for the analysis of nonlinear mixed effects models (NLMEMs). Nonlinear mixed effects models are widely used to analyze longitudinal data collected in clinical studies and for their ability to quantify several levels of variability, to handle unbalanced data, and to identify individual specific covariates. It is possible to define prior distribution models on the fixed effects. The following nonlinear mixed effects model for continuous outputs is considered:

$$y_{ij} = f(t_{ij}, \psi_i) + \epsilon_{ij} \qquad 1 \le i \le N\ , 1 \le j \le n_i$$

where $f(t_{ij}, \psi_i)$ is predicted by the model at time t_{ij}, ψ_i is the vector of parameters for subject i, and e_{ij} is a residual Gaussian error term of constant SD. In Monolix, we assume that ψ_i is a transformation of a Gaussian random vector.

Through fitting Model (1) to the clinical trial data, confidence intervals for each fitted parameter can be determined. Confidence intervals are determined by the Monolix software based on the standard errors derived from an estimation of the Fisher Information Matrix on the profile likelihood [30].

3. Results

The resulting parameter fit of Model (1) to the 45-μg two-dose clinical trial data, and its corresponding simulations of are shown in Fig. 2 (also see Supplementary Material, FigureS2). The fitted parameter values are listed in Table 1, including confidence intervals determined by the Monolix fitting routine. We note that over time, we observe an increase to a peak value in all population variables, followed by a decay, but that the peak times can vary considerably between populations. Please see the Th1 and IL4 dynamics in Fig. 3, for example. Additionally, under the fitted parameter values listed in Table 1, the model decays to a natural equilibrium of the Th1, Th2, F, I4, CTL, A and B populations in absence of vaccine. As the fitted model parameters are associated with data between days 0 and 60 post dose one and there are no measurements of the immune system prior to vaccination, it is not possible to interpret this equilibrium in terms of the underlying biology both prior to vaccination and over a long timeframe post dose two. Basal levels of interferon, interleukin, and Th1 and Th2 cytokines do exist in absence of immune system antigen stimulation [31–33]. An in-depth analysis is left to future work when longer term measurements of the immune system are available. Herewithin, we report results in the short-term post vaccination up to day 120 post dose one (and only two months post final measurement in the clinical trial).

An antibody-mediated response is referred to as humoral immunity. We find humoral immunity degradation rates, γ_a and γ_b to be 0.90 and 0.05 d^{-1} respectively. We predict that the vaccine elicited antibody levels will decay to 23% of the peak magnitude by day 120.

Fig. 3 shows that a balance between the T_H1 and T_H2 immune responses is achieved — Th1 cytokines peak early and this is followed by a peak in Th2 cytokines sometime later, but with much lower magnitude. This outcome is in agreement with [34] whereby a balance is struck between IFN_γ and IL-4 such that the former dominates the immune response — we observe lesser enhancement of type 2 cytokines (i.e., IF-4) in comparison with type 1 cytokines (i.e., IFN_γ), and a balanced T_H1-T_H2 profile results. We note that this result reflects the inhibitory activities of the T_H1 and T_H2 arms of the immune response. Each of the two helper T cell subsets inhibit the development and function of the other. IFN_γ, produced by T_H1 cells, inhibits the development and function of T_H2 cells, whereas IL-4, produced by T_H2 cells, inhibits the development and function of T_H1 cells. Presumably, the reason T_H1 and T_H2 cells inhibit each other is that both subsets also induce inflammation, which must be regulated. The T_H1-T_H2 balance observed here indicates that a pro-inflammatory response is elicited by the M59 subunit vaccine.

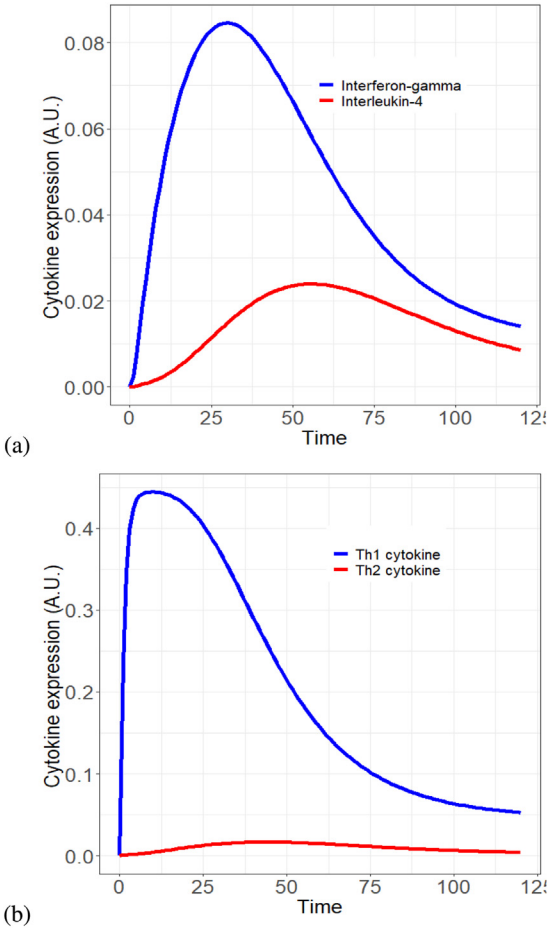

Fig. 3. (a) Predicted IFN$_\gamma$ and IL-4 based on fits to clinical data for two doses of MF59-adjuvanted subunit vaccine for COVID-19. (b) Predicted T_H1 and T_H2 cytokines as a function of time.

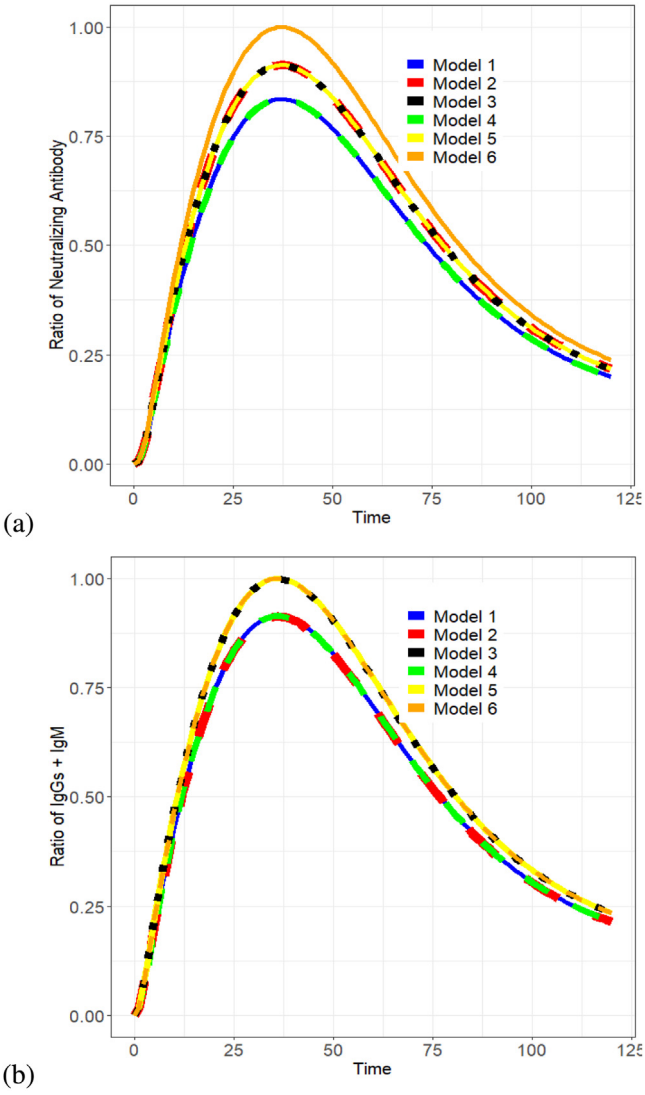

Fig. 4. (a) Ratio of predicted neutralizing antibody normalized by peak neutralizing antibody (b) Ratio of predicted Ig-multiplex, normalized by peak Ig-multiplex.

We extend our study on the effects of vaccine adjuvants in Fig. 4, which plots the predicted neutralizing and Ig-multiplex antibodies for Models (1)–(6). Both subplots are normalized by the peak magnitude resulting from Model (1) (blue lines). Adding an adjuvant to the antibody response increases the neutralizing antibody and Ig-multiplex responses in different manners, depending on the model structure being considered (see Models (2)–(6)). The highest neutralizing antibody ratio belongs to the Model (6) (yellow line) which adds adjuvanted enhancement in all antibody production terms. However, the Ig-multiplex responses in Fig. 4 (bottom panel) shows that enhanced activity in the production of [B] is only needed to achieve a maximal Ig-multiplex response (Model (3), black line).

It is interesting to note that Model (4) does not achieve any augmentation in neutralizing or Ig-multiplex antibodies compared to Model (1). This result and that above show that augmentations in T_H1 activity are needed to enhance antibody activity — enhancing T_H2 antibody production alone, has no effect on these outcomes.

3.1. Sensitivity and uncertainty analysis

Sensitivity and uncertainty analysis is used to identify model parameters that most affect immunity outcomes within their defined parameter ranges. Here, we utilize the robust Latin Hypercube Sampling and Partial rank correlation coefficient method (LHS-PRCC) [35] to identify model parameters that most affect antibody, T_H1, and T_H2 peak magnitudes and loss from the peak (we have chosen to look at loss from 100 to 92% of peak value as this is what has been considered in previous studies [36]). LHS-PRCC results are shown in Figs. 5 and 6. We used a sample size of 10000 parameter sets determined using a latin hypercube within the defined ranges of the parameter values shown in Table 1. Monotonic relationships between the outcomes of interest (peak magnitude of antibodies, T_H1 and T_H2 populations) and all model parameters were verified. LHS-PRCC results greater |0.5| are considered significant. These are listed in Table 2.

Considering both the peak and loss of immunity sensitivity analysis results, we find that, common to both sensitivity analysis results, to increase all peak values and decrease all immunity loss, decreases in γ_v are needed, as well as increases in η_{th1}. In other words, based on the sensitivity analysis results of the peak and loss of immunity, both sensitivity analyses are in direct correlation with each other. This demonstrates that the T_H1 response has the strongest influence on Eq. (1) outcomes.

3.2. Vaccine dose size

In order to be an effective mitigation tool, all vaccines should produce a strong immune response. In the Supplementary Material, we plot the outcomes of the model fitting to the clinical trial data related to two $15\mu_g$ doses. Corresponding parameter values are also listed in the

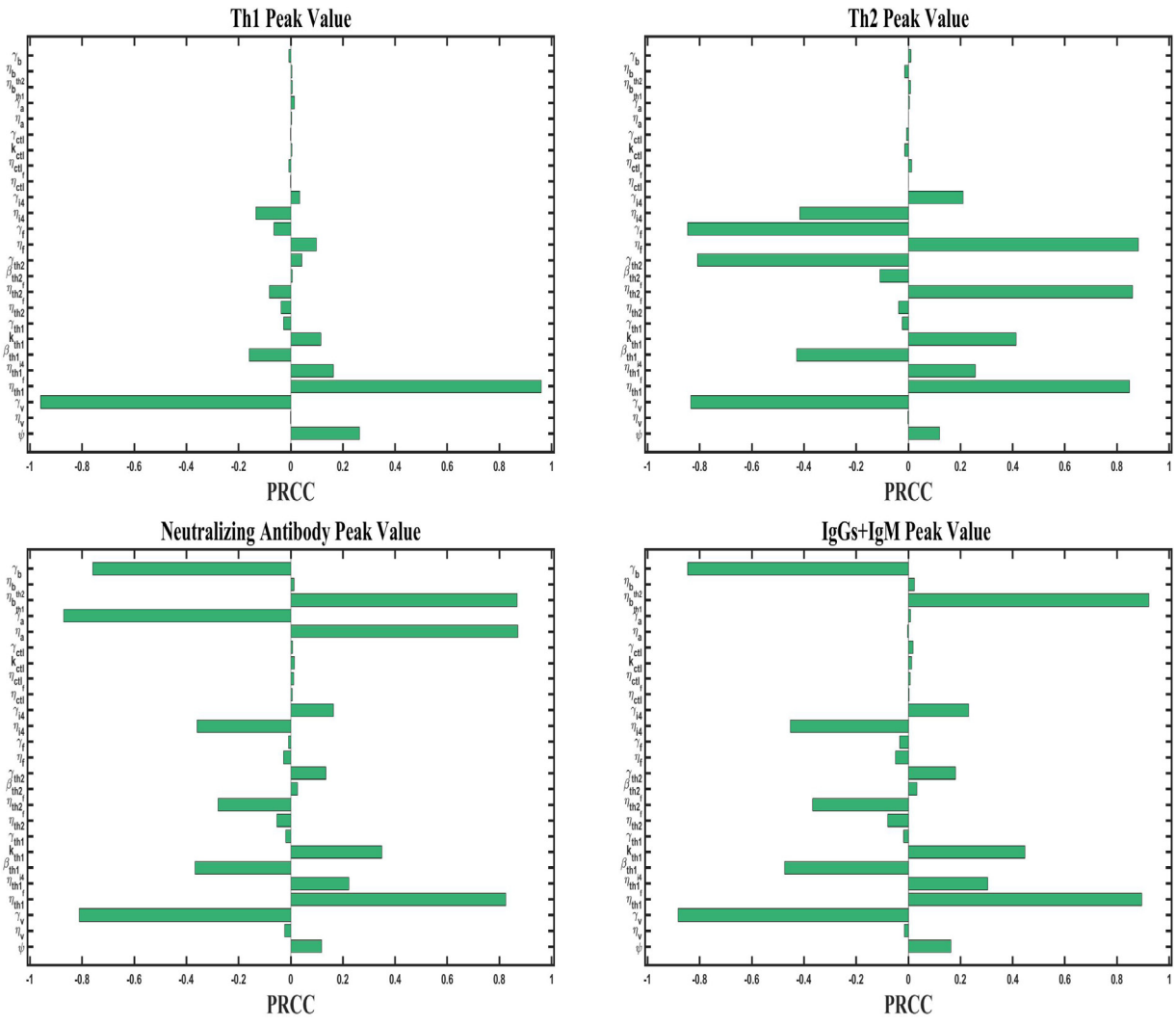

Fig. 5. Sensitivity analysis of T_H1-cytokine, T_H2-cytokine, Neutralizing antibody and Ig-multiplex population to changes in parameters of model (1).

Table 2
PRCC values for parameters of model (1) that significantly affect peak value or loss rate.

	Peak value			Immunity loss		
Variable	Parameter	Magnitude	Correlation	Parameter	Magnitude	Correlation
T_H1	γ_v	0.96	−	γ_v	0.74	+
	η_{th1}	0.96	+	$\beta_{th1_{i4}}$	0.66	−
				η_{i4}	0.65	−
				η_{th1}	0.64	−
				k_{th1}	0.62	+
				η_{th2_f}	0.61	−
				η_f	0.57	−
IgGs + IgM (Ig-multiplex)	$\eta_{b_{th1}}$	0.92	+	$\beta_{th1_{i4}}$	0.64	−
	η_{th1}	0.89	+	η_{i4}	0.6	−
	γ_v	0.88	−	η_{th1}	0.59	−
	γ_b	0.84	−	k_{th1}	0.59	+
				η_{th2_f}	0.58	−
				γ_v	0.55	+
				γ_b	0.5	−
				γ_{i4}	0.5	+
T_H2	η_f	0.88	+	$\beta_{th1_{i4}}$	0.6	−
	η_{th2_f}	0.86	+	η_{th1}	0.56	−
	η_{th1}	0.85	+	k_{th1}	0.56	+
	γ_f	0.85	−	η_{th2_f}	0.56	−
	γ_v	0.83	−	η_{i4}	0.56	−
	γ_{th2}	0.81	−	γ_v	0.5	+
				γ_{i4}	0.5	+

(*continued on next page*)

Table 2 (*continued*).

Variable	Peak value			Immunity loss		
	Parameter	Magnitude	Correlation	Parameter	Magnitude	Correlation
Neutralizing Antibody	η_a	0.87	+	k_{th1}	0.6	+
	γ_a	0.87	–	$\beta_{th1_{i4}}$	0.6	–
	$\eta_{b_{th1}}$	0.87	+	η_{i4}	0.59	–
	η_{th1}	0.83	+	η_{th1}	0.59	–
	γ_v	0.81	–	η_{th2_f}	0.58	–
	γ_b	0.76	–	γ_v	0.55	+
				γ_{i4}	0.5	+
				γ_b	0.5	–

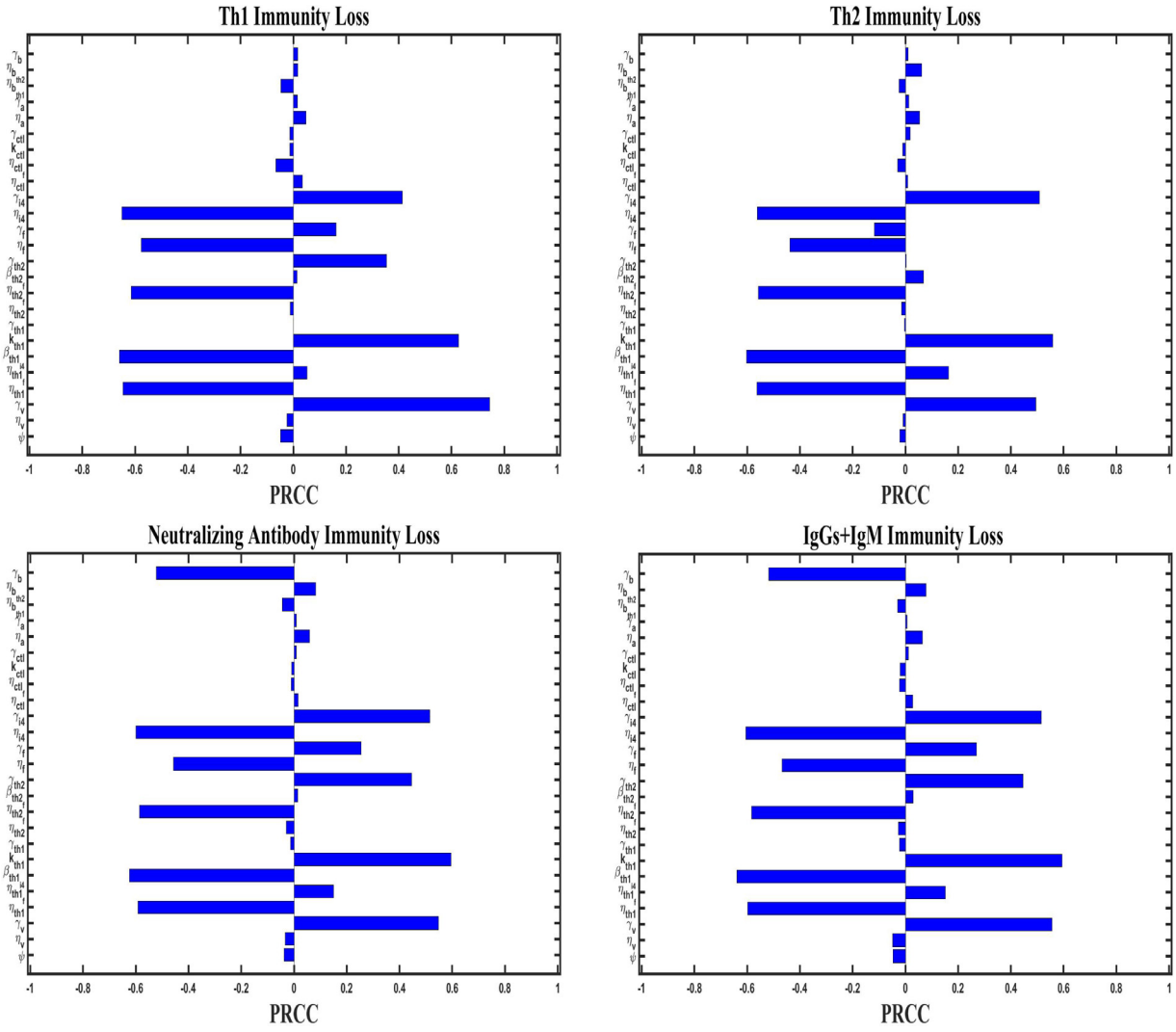

Fig. 6. LHS sensitivity of immunity loss of T_H1-cytokine, T_H2-cytokine, Neutralizing antibody and Ig-multiplex population to changes in parameters of model, 8% loss from the peak.

supplementary. We note that many of the fitted parameter values are similar in magnitude to the $55\mu_g$ two dose clinical trial fitted values. However, while γ_v is reduced, η_{th1} is also reduced. Additionally, there are changes in many parameters that will decrease peak values and increase immunity loss. We therefore find that the two $15\mu_g$ doses of vaccine will be sub-optimal in eliciting an effective immune response, especially compared to two $45\mu_g$ doses.

Fig. 7 plots the outcome of our model assuming different initial doses of the vaccine, assuming the parameter values related to the $45\mu_g$ two dose clinical trial data (see Table 1). Specifically, we plot the neutralizing and Ig-multiplex antibody populations. Intuitively, the outcomes depend on the dose size. Overall, we find that two doses of 5 and 15 μg MF59-adjuvanted protein vaccine elicit lower peak immunity responses against SARS-CoV-2. However, we observe that each vaccine dosage example will move to similar measurements of the neutralizing and Ig-multiplex antibody populations by day 120. We note that if the goal of vaccination is longer term persistence of neutralizing and Ig-multiplex antibodies, given the parameter value assumptions here, a smaller dose size would allow for more individuals to be vaccinated. However, this is not typically the case — high population levels of antibodies are typically wanted in the short-term to provide optimal

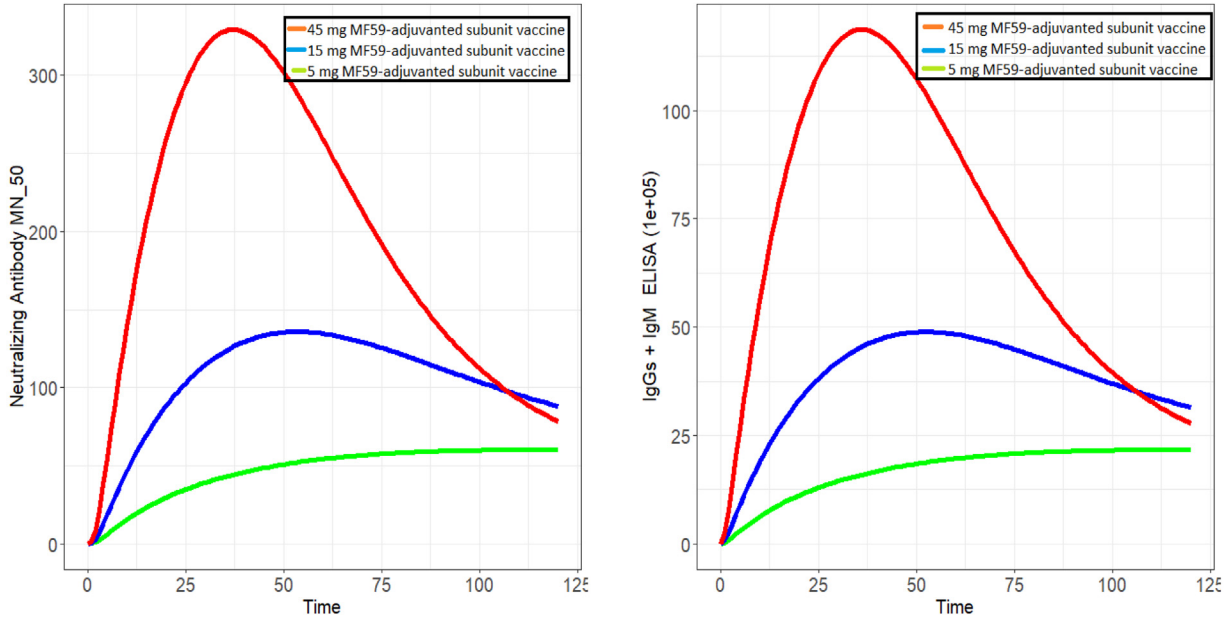

Fig. 7. Neutralizing and Ig-multiplex dynamics as a function of time for 5, 15 and 45 μg MF59-adjuvanted subunit vaccine dose sizes. Parameter values are from Table 1.

protection. Studies on the protective capacity of the levels of antibody predicted by our mathematical model need to be conducted.

4. Discussion

Subunit vaccines contain purified viral proteins (an antigen) that are not infectious, and often also contain an adjuvant. Protein subunit candidates usually exhibit an extremely favorable safety profile but require an adjuvant which is used precisely to enhance cell mediated immune responses. In this study, we developed a mathematical model of immune system activation by a protein subunit adjuvanted vaccine. The model was developed considering the documented effects of the M59-adjuvant on the T_H1 and T_H2 arms of the immune response [4]. We fit the mathematical model to clinical trial data from [4] using a 45 μg dose size. The model projects an increase in immune system activity, followed by a decrease. We observe a balance between T_H1 and T_H2 cytokines, and find a TH1 dominated response overall. Sensitivity analysis demonstrates that peak immune system outcomes are most affected by changes in T_H1 immune system activation parameters. Finally, we find that, if smaller dose sizes of the vaccine have the same capability in activating the immune response, peak responses can be considerably lower, which is not generally a wanted outcome of vaccination.

Inflammatory and anti-inflammatory signals can affect a host's severity of infection [37–39]. In the SARS-CoV-2 sclamp vaccine, M59 is used as an adjuvant. M59 is known to elicit higher T_H1 (humoral) and T_H2 (cellular) immune responses. The adjuvant MF59 is also known to primarily enhance T_H1 responses. Fig. 3 shows that T_H1 cytokine expression exceeds that of T_H2 cytokines. Our T_H1 and T_H2 predictions are in agreement with the AS03-adjuvanted subunit vaccine [40]. The balanced production of cytokines associated with T_H1 and T_H2 responses may be advantageous in boosting T-cell protection. The balance may also reduce the severity of respiratory disease outcome [41].

In the M59-adjuvanted protein subunit vaccine clinical trial, antibodies were induced against the S1, S2, and receptor binding domain spike glycoprotein subdomains, as well as the clamp domain [4]. We considered an analysis of neutralizing antibodies and the Ig-multiplex. We find peak Ig-multiplex response at day 36. The neutralizing antibody maximum is at day 37. Thus, maximum antibody value is achieved approximately five weeks after the first vaccine dose. In this work, we also study the half maximum of antibody titres to characterize the percent loss. The Ig-multiplex half-maximum is reached at day 80 and that of the neutralizing antibody appears at day 82. The model predicts that the protein subunit vaccine maintains approximately 23% of the neutralizing antibody and Ig-multiplex by day 120. A recent study proposed that relatively low antibody titres are sufficient for protection against SARS-CoV-2 in rhesus macaques, with approximately 8% from peak needed to protect the host from infection [36]. However, such clinical evidence for humans is still absent.

We have included the adjuvant effect using the same parameter ψ in Models (1)–(6). This analysis was used to determine models where added adjuvant effects (i.e., what model terms) would be needed to increase peak outcomes of immunity. We find that Model (6) performs best considering neutralizing antibodies, but that IgG and IgM are maximized for Model (3),(5),(6), showing that enhancement of η_{bth1} is needed. We note that, for simplicity, the effect of the adjuvant was considered the same in all model terms. The effect of the adjuvant, however, can vary between the modeled mechanisms. A more fine-grained study of the adjuvant is planned for future work.

We can also compare our model-determined values with similar values from the literature. For example, in this work we find an IL-4 clearance rate of 0.09 d^{-1}. A previous SARS-CoV-2 infection study determined an IL-2 degradation of 0.096 d^{-1} [1], and further, an average interleukin degradation rate of 0.027 d^{-1} was found in our previous work on mRNA vaccines [1]. We also find a CD8+ clearance rate of 0.026 d^{-1}, leading to an equivalent half life of 26.7 days. This value is of similar magnitude to other previously reported values. For example, CD8+ decay rate of 0.01 with an equivalent half life of 69 days was determined for severe H7N9 disease [42].

Recently, we studied antibody decay from peak level for other COVID-19 vaccine platforms [1–3]. Table 3 summarizes results from these and the current study. Considering these results, it appears that the adenovirus-based Oxford vaccine and the MF59-adjuvanted subunit vaccine have more gradual declines in antibody. However, a more detailed modeling study on a comprehensive dataset for all vaccines with similar measurement units is needed to make a full comparison. This is considered for future work.

5. Data sharing

In the supplementary material, all individual fitted plots to the two-dose MF59-adjuvanted spike glycoprotein-clamp vaccine are available.

Table 3
Comparison of antibody degradation for 3 vaccine types..

Vaccine type	25% loss (day)	50% loss (day)	75% loss (day)
Two-dose 45 μg MF59-adjuvanted spike protein vaccine	60	80	116
Two standard dose BNT162b2	72	88	110
Two-dose adenovirus-based Oxford vaccine	115	138	178

The raw data used for fitting can be made available upon reasonable request to the corresponding author.

CRediT authorship contribution statement

Samaneh Gholami: Conceived the study and developed the model, Conducted model fitting and analysis, Writing – original draft. **Mohammad Sajjad Ghaemi:** Conceived the study and developed the model, Writing – original draft. **Hsu Kiang Ooi:** Conceived the study and developed the model, Writing – original draft. **Jane M. Heffernan:** Conceived the study and developed the model, Writing – original draft.

Declaration of competing interest

The authors declare that they have no known competing financial interests or personal relationships that could have appeared to influence the work reported in this paper.

Data availability

Data will be made available on request.

Acknowledgments

We thank the Canadian In-Host Modeling Group (Matt Betti, Dan Coombs, Thomas Hillen, Jude Kong, Kang Ling Liao, Nicole Mideo, Stephanie Portet, Angie Raad, Lindi Wahl, James Watmough) for fruitful discussions. All authors have read and agreed to the published version

Funding

This research is supported by NSERC Discovery Grant, CIHR-Fields COVID Immunity Task Force, Canada, NRC Pandemic Response Challenge Program, Canada Grant No. PR016-1.

Appendix A. Supplementary data

Supplementary material related to this article can be found online at https://doi.org/10.1016/j.mbs.2023.108970.

References

[1] Chapin S. Korosec, Suzan Farhang-Sardroodi, David W. Dick, Samaneh Gholami, Mohammad Sajjad Ghaemi, Iain R. Moyles, Morgan Craig, Hsu Kiang Ooi, Jane M. Heffernan, Long-term predictions of humoral immunity after two doses of BNT162b2 and mRNA-1273 vaccines based on dosage, age and sex, Sci. Rep. 12 (1) (2022) 1–15.

[2] Iain R. Moyles, Chapin S. Korosec, Jane M. Heffernan, Determination of significant immunological timescales from mRNA-LNP-based vaccines in humans, MedRxiv 2022.07.25 (2022) http://dx.doi.org/10.1101/2022.07.25.22278031, arXiv:2022.07.25.22278031.

[3] Suzan Farhang-sardroodi, Chapin S. Korosec, Samaneh Gholami, Morgan Craig, Iain R. Moyles, Mohammad Sajjad Ghaemi, Hsu Kiang Ooi, Jane M. Heffernan, Analysis of host immunological response of adenovirus-based COVID-19 vaccines, Vaccines 9 (8) (2021) 861.

[4] Keith J. Chappell, Francesca L. Mordant, Zheyi Li, Danushka K. Wijesundara, Paula Ellenberg, Julia A. Lackenby, Stacey T.M. Cheung, Naphak Modhiran, Michael S. Avumegah, Christina L. Henderson, et al., Safety and immunogenicity of an MF59-adjuvanted spike glycoprotein-clamp vaccine for SARS-CoV-2: a randomised, double-blind, placebo-controlled, phase 1 trial, Lancet Infect Dis (2021).

[5] Nak-Hyung Lee, Jung-Ah Lee, Seung-Yong Park, Chang-Seon Song, In-Soo Choi, Joong-Bok Lee, A review of vaccine development and research for industry animals in Korea, Clin. Exp. Vaccin. Res. 1 (1) (2012) 18–34.

[6] Abhishek Vartak, Steven J. Sucheck, Recent advances in subunit vaccine carriers, Vaccines 4 (2) (2016) 12.

[7] Rajesh K. Gupta, Edgar H. Relyveld, Erik B. Lindblad, Bernard Bizzini, Shlomo Ben-Efraim, Chander Kanta Gupta, Adjuvants—a balance between toxicity and adjuvanticity, Vaccine 11 (3) (1993) 293–306.

[8] J.Y. Tai, P.P. Vella, A.A. McLean, A.F. Woodhour, W.J. McAleer, A. Sha, C. Dennis-Sykes, M.R. Hilleman, Haemophilus influenzae type b polysaccharide-protein conjugate vaccine, Proc. Soc. Exp. Biol. Med. 184 (2) (1987) 154–161.

[9] Ronald W. Ellis, New technologies for making vaccines, Vaccine 17 (13–14) (1999) 1596–1604.

[10] T. Wuorimaa, H. Käyhty, Current state of pneumococcal vaccines, Scand. J. Immunol. 56 (2) (2002) 111–129.

[11] Kim Kristensen, Anette Gyhrs, Birgitte Lausen, Torben Barington, Carsten Heilmann, Antibody response to Haemophilus influenzae type b capsular polysaccharide conjugated to tetanus toxoid in preterm infants, Pediatr. Infect. Dis. J. 15 (6) (1996) 525–529.

[12] Andreas Handel, Laura E. Liao, Catherine A.A. Beauchemin, Progress and trends in mathematical modelling of influenza A virus infections, Curr. Opin. Syst. Biol. 12 (2018) 30–36.

[13] William E. Paul, Robert A. Seder, Lymphocyte responses and cytokines, Cell 76 (2) (1994) 241–251.

[14] Shizuo Akira, Tadamitsu Kishimoto, IL-6 and NF-IL6 in acute-phase response and viral infection, Immunol. Rev. 127 (1992) 25–50.

[15] S.R. Paludan, Interleukin-4 and interferon-gamma: the quintessence of a mutual antagonistic relationship, Scand. J. Immunol. 48 (5) (1998) 459–468.

[16] Jason R. Lees, Interferon gamma in autoimmunity: A complicated player on a complex stage, Cytokine 74 (1) (2015) 18–26.

[17] Todd N. Eagar, Stephen D. Miller, 16 - Helper T-cell subsets and control of the inflammatory response, in: Robert R. Rich, Thomas A. Fleisher, William T. Shearer, Harry W. Schroeder, Anthony J. Frew, Cornelia M. Weyand (Eds.), Clinical Immunology, fifth ed., Elsevier, London, 2019, pp. 235–245.e1.

[18] Allen Wensky, Maria Cecília Garibaldi Marcondes, Juan J. Lafaille, The role of IFN-γ in the production of Th2 subpopulations: implications for variable Th2-mediated pathologies in autoimmunity, J. Immunol. 167 (6) (2001) 3074–3081.

[19] Piyali Chatterjee, Valorie L. Chiasson, Kelsey R. Bounds, Brett M. Mitchell, Regulation of the anti-inflammatory cytokines interleukin-4 and interleukin-10 during pregnancy, Front. Immunol. 5 (2014) 253.

[20] Kaviyarasi Renu, Mohana Devi Subramaniam, Rituraj Chakraborty, Myakala Haritha, Mahalaxmi Iyer, Geetha Bharathi, Siva Kamalakannan, Vellingiri Balachandar, V.G. Abilash, The role of interleukin-4 in COVID-19 associated male infertility–a hypothesis: running title: IL-4 and its role in COVID-19 associated male infertility, J. Reprod. Immunol. (2020) 103213.

[21] Moises Santillán, On the use of the hill functions in mathematical models of gene regulatory networks, Math. Model. Nat. Phenom. 3 (2) (2008) 85–97.

[22] Roald Nezlin, The Immunoglobulins: Structure and Function, Academic Press, 1998.

[23] Harry W. Schroeder Jr., Lisa Cavacini, Structure and function of immunoglobulins, J. Allergy Clin. Immunol. 125 (2) (2010) S41–S52.

[24] Bruce Alberts, Alexander Johnson, Julian Lewis, Martin Raff, Keith Roberts, Peter Walter, et al., Molecular biology of the cell, Scand. J. Rheumatol. 32 (2) (2003) 125.

[25] Davide F. Robbiani, Christian Gaebler, Frauke Muecksch, Julio C.C. Lorenzi, Zijun Wang, Alice Cho, Marianna Agudelo, Christopher O. Barnes, Anna Gazumyan, Shlomo Finkin, et al., Convergent antibody responses to SARS-CoV-2 in convalescent individuals, Nature 584 (7821) (2020) 437–442.

[26] Brien K. Haun, Chih-Yun Lai, Caitlin A. Williams, Teri Ann S. Wong, Michael M. Lieberman, Laurent Pessaint, Hanne Andersen, Axel T. Lehrer, CoVaccine HT™ adjuvant potentiates robust immune responses to recombinant SARS-CoV-2 spike S1 immunization, Front. Immunol. 11 (2020) 2780.

[27] Takashi Kuribayashi, Elimination half-lives of interleukin-6 and cytokine-induced neutrophil chemoattractant-1 synthesized in response to inflammatory stimulation in rats, Lab. Animal Res. 34 (2) (2018) 80–83.
[28] John A. Hangasky, Thomas A. Waldmann, Daniel V. Santi, Interleukin 15 pharmacokinetics and consumption by a dynamic cytokine sink, Front. Immunol. 11 (2020) 1813.
[29] Lorelie H. Villarete, Daniel G. Remick, Transcriptional and post-transcriptional regulation of interleukin-8, Am. J. Pathol. 149 (5) (1996) 1685.
[30] Monolix, 2019.
[31] Mohamad S. Hakim, Sunrui Chen, Shihao Ding, Yuebang Yin, Aqsa Ikram, Xiaoxia Ma, Wenshi Wang, Maikel P. Peppelenbosch, Qiuwei Pan, Basal interferon signaling and therapeutic use of interferons in controlling rotavirus infection in human intestinal cells and organoids, Sci. Rep. 8 (1) (2018) 1–13.
[32] Jean Francois Viallard, J.L. Pellegrin, V. Ranchin, T. Schaeverbeke, J. Dehais, M. Longy-Boursier, J.M. Ragnaud, B. Leng, J.F. Moreau, Th1 (IL-2, interferon-gamma (IFN-γ)) and Th2 (IL-10, IL-4) cytokine production by peripheral blood mononuclear cells (PBMC) from patients with systemic lupus erythematosus (SLE), Clin. Exp. Immunol. 115 (1) (1999) 189–195.
[33] Danilo Bretas de Oliveira, Gabriel Magno de Freitas Almeida, Antônio Carlos Martins Guedes, Flávia Patrícia Sena Teixeira Santos, Claudio Antônio Bonjardim, Paulo César Peregrino Ferreira, Erna Geessien Kroon, Basal activation of type I interferons (Alpha2 and beta) and OAS genes: Insights into differential expression profiles of interferon system components in systemic sclerosis, Int. J. Rheumatol. 2011 (2011).
[34] U. Boehm, T. Klamp, M. Groot, J.C. Howard, Cellular responses to interferon-γ, Annu. Rev. Immunol. 15 (1) (1997) 749–795.
[35] Boloye Gomero, Latin hypercube sampling and partial rank correlation coefficient analysis applied to an optimal control problem, 2012.
[36] Katherine McMahan, Jingyou Yu, Noe B. Mercado, Carolin Loos, Lisa H. Tostanoski, Abishek Chandrashekar, Jinyan Liu, Lauren Peter, Caroline Atyeo, Alex Zhu, et al., Correlates of protection against SARS-CoV-2 in rhesus macaques, Nature 590 (7847) (2021) 630–634.
[37] Jun Chen, Yuk Fai Lau, Elaine W. Lamirande, Christopher D. Paddock, Jeanine H. Bartlett, Sherif R. Zaki, Kanta Subbarao, Cellular immune responses to severe acute respiratory syndrome coronavirus (SARS-CoV) infection in senescent BALB/c mice: CD4+ T cells are important in control of SARS-CoV infection, J. Virol. 84 (3) (2010) 1289–1301.
[38] Jincun Zhao, Jingxian Zhao, Stanley Perlman, T cell responses are required for protection from clinical disease and for virus clearance in severe acute respiratory syndrome coronavirus-infected mice, J. Virol. 84 (18) (2010) 9318–9325.
[39] David C. Fajgenbaum, Carl H. June, Cytokine storm, N. Engl. J. Med. 383 (23) (2020) 2255–2273.
[40] Prabhu S. Arunachalam, Alexandra C. Walls, Nadia Golden, Caroline Atyeo, Stephanie Fischinger, Chunfeng Li, Pyone Aye, Mary Jane Navarro, Lilin Lai, Venkata Viswanadh Edara, et al., Adjuvanting a subunit COVID-19 vaccine to induce protective immunity, Nature 594 (7862) (2021) 253–258.
[41] Abi Berger, Th1 and Th2 responses: what are they? Bmj 321 (7258) (2000) 424.
[42] Zhongfang Wang, Yanmin Wan, Chenli Qiu, Sergio Quinones-Parra, Zhaoqin Zhu, Liyen Loh, Di Tian, Yanqin Ren, Yunwen Hu, Xiaoyan Zhang, et al., Recovery from severe H7N9 disease is associated with diverse response mechanisms dominated by CD8+ T cells, Nature Commun. 6 (1) (2015) 1–12.